

Fluorescent sensing and determination of mercury (II) ions in water

Phendukani Ncube, Rui WM Krause, Derek T Ndinteh and Bhekishe Mamba*

Department of Applied Chemistry, University of Johannesburg, PO Box 17011, Doornfontein 2028, South Africa

ABSTRACT

The presence of heavy metals released from industrial activities into water streams is an ever-growing challenge to ensuring a safe and clean aquatic environment. Detection and determination of the levels of these heavy metals in wastewater is an important step before any measures can be taken. In this study we report on a fluorescent sensing probe based on a naphthyl azo dye modified dibenzo-18-crown-6-ether (DB18C6) for the detection and determination of mercury (II) ions in water. The probe showed high sensitivity and selectivity towards the mercury (II) ion among various alkali, alkaline earth, and transition metal ions. The mercury (II) ion quenched the fluorescence of the probe. Stern-Volmer quenching constants (K_{sv}) were found to be highest for Hg^{2+} ion at $1.18 \times 10^5 M^{-1}$ compared to $3.85 \times 10^4 M^{-1}$ for copper (II) ion. The stoichiometry of the sensor-metal ion interaction was found to be 1:1 for both metal ions using Job plots. The detection limit for Hg^{2+} was $1.25 \times 10^{-8} M$. The dye modified crown ether was then used to detect mercury in a water sample from a coal-fired power plant and to determine the amount of mercury in the water sample.

Keywords: azo dye, crown ether, fluorescence, mercury (II), sensor, water

INTRODUCTION

The detection of heavy metals in polluted environments is an ever-growing concern and is the subject of ongoing research in various research groups. Of the toxic heavy metals, mercury is one of the highly toxic, leading to diseases such as acrodynia (pinks disease), Hunter-Russell syndrome and Minamata disease (Fujiki and Tajima, 1992; He et al., 2009; Kudo et al., 1988). Health problems associated with mercury are made worse due to its accumulative and persistent nature in the environment and in living organisms. Mercury is released into water by industrial processes such as coal burning and natural causes like volcanic eruptions (Yari and Papi, 2009). South Africa has been reported as the second highest emitter ($50 t\text{-year}^{-1}$) of Hg in the world, after China (Pacyna et al., 2006), even though later estimates dispute this high emission rate and place emissions in the range of $2.6\text{--}17.6 t\text{-year}^{-1}$ (Dabrowski et al., 2008). South Africa is the third-largest coal producer in the world, with coal accounting for 64% of SA's energy supply. Electricity generation is responsible for 61% of total coal combustion. About 93% of SA's electricity is produced from coal-fired power plants (Dabrowski et al., 2008). South African coal Hg content ranges from 0.04 to $0.25 mg\ell^{-1}$. This extensive use of coal in electricity generation means large amounts of Hg are released annually into South African water and the atmosphere.

There are existing methods for the determination and detection of Hg^{2+} ions, including atomic absorption spectroscopy (AAS) (Martinis et al., 2009), inductively coupled plasma spectroscopy (ICP) (Passariello et al., 1996), molecular absorption spectroscopy (Yang et al., 2010) and electro-analytical

techniques (Abu-Shawish, 2009; Khani et al., 2010). While these methods are well established, they often require significant sample preparation and expensive laboratory-based instruments. Recent analytical interest in optical methods such as fluorescence spectroscopy could offer alternative rapid methods for metal screening in the field.

Fluorescent chemosensors have received a lot of attention due to their high sensitivity, selectivity, simplicity, low cost instrumentation and field-work applicability (Kondo et al., 2011; Moczar et al., 2010). The design of these chemosensors for metal ion detection often consists of a receptor ligand (such as crown ether) and a fluorophore, often naphthyl, anthracene or pyrene groups, as the signalling unit (Chen et al., 2009; Fakhari et al. 1997; Hsieh et al., 2009). The basis of detection is often the photo-induced charge transfer (PET) effect, that is, the electron transfer between the receptor part and the fluorophore when a metal ion is bound, which results in the quenching of fluorescence. In our previous work we reported on a fluorescent chemosensor bearing an azo dye modified cyclodextrin for the sensing of chlorophenols (Ncube et al., 2011). Fluorescent mercury (II)-selective chemosensors, bearing a crown ether moiety as the metal ligand and a fluorophore for signalling, have been documented (Guo et al., 2004), and those that show simultaneous response to both mercury (II) and copper (II) (Lee et al., 2009) or mercury (II) and lead (II) (Kiwan et al., 1997) have also been reported. Improvement of these chemosensors in terms of selectivity, sensitivity and lower detection limits remains a challenge, hence the need to design new ones.

These sensors have found a wide range of application, including detection of metal ions in water (Yari and Papi, 2009), in biological media (He et al., 2009) and in organic media (Hsieh et al., 2009). The difficulty in selectively detecting heavy metals in water is their high water of hydration and the fact that most fluorescent probes are quenched by several metal ions (Guo et al., 2004). It therefore remains a challenge to find a chemosensor that can selectively respond to one heavy

* To whom all correspondence should be addressed.

+27 11 559 6156; Fax: +27 11 559 6425;
e-mail: bmamba@uj.ac.za

Received 21 January 2013; accepted in revised form 17 December 2013.

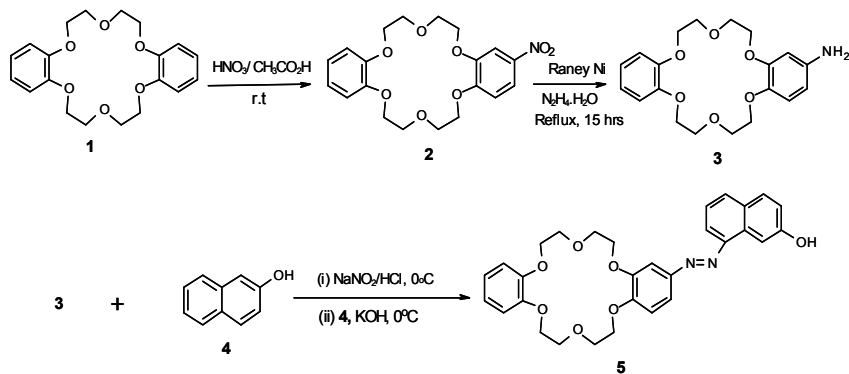


Figure 1
Synthetic pathway to
DB18C6 azo dye 5

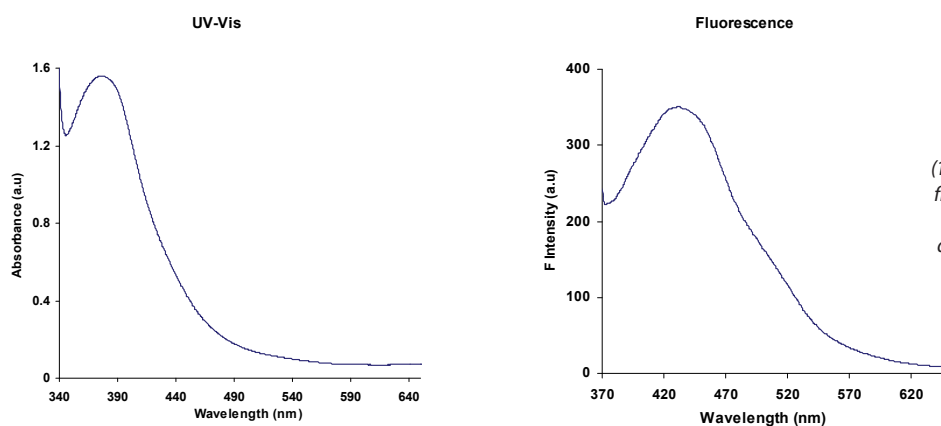


Figure 2
(a) UV-Vis spectrum
(1:1 MeOH/H₂O) and (b)
fluorescence spectrum
($\lambda_{exc} = 355$ nm) of the
dye-modified DB18C6

metal ion. In this work we report on a naphthyl azo dye modified dibenzo-18-crown-6 ether as a potential fluorescent probe for the selective detection of mercury (II) in aqueous media, and in water samples collected near a South African coal-fired power station, where mercury is likely to be released in large quantities.

EXPERIMENTAL

Materials and apparatus

All reagents and solvents were obtained from Sigma-Aldrich (Germany) unless otherwise stated. Reagents were analytical grade and were used without further purification. Absorption spectra were recorded on a Shimadzu UV-2450 UV-VIS Spectrophotometer at room temperature. Fluorescence measurements were done on a Perkin Elmer LS45 Fluorescence Spectrometer with excitation and emission slit widths of 10.0 nm, respectively, a scan speed of 150 nm·min⁻¹ from 200 nm to 650 nm, and an excitation wavelength of 355 nm. Infrared spectra were taken on a Perkin Elmer Spectra100 ATR-FT-IR Spectrometer whereas ¹H- and ¹³C-NMR spectroscopy was performed using a 400 MHz Bruker Avance Spectrometer. CHNS elemental analysis was done on an elemental analyser. Mass spectra were recorded on a Waters Synapt G2 ESI-MS instrument with calibration performed using sodium formate.

Synthesis of naphthyl-azo modified dibenzo-18-crown-6 ether 5

The azo dye modified dibenzo-18-crown-6 fluorophore was synthesised according to previously reported methods (Grebenyuk et al., 2000; Pandya and Agrawal, 2002) with

slight modifications. Starting from DB18C6 (**1**) (1.054 g, 2.9 mmol) the first step was nitration, then reduction and finally diazo coupling with β -naphthol (**4**) to give the final product (**5**) (Fig. 1) as a deep red solid. Yield: 0.846 g, 55%; mp: 261–263°C (Lit. mp. 260°C; Pandya and Agrawal, 2002); UV/Vis. (1:1 H₂O/MeOH): $\lambda_{max} = 380$ nm; FT-IR: ν (cm⁻¹): 3 265 (OH stretch); 3 053 (CH stretch); 1 629 (C=C stretch); 1 600 (N-H bending); 1 275 (Ar-O stretch); 1 241 (C-O-C stretch) ¹H-NMR (CDCl₃) (Fig. 2); δ (mg l⁻¹): 7.85 (1H, dd, 5'-H); 7.64 (1H, d, 3'-H); 6.81 (5H, s, 6'-, 3''-, 4''-, 5''-, and 6''- H); 4.05–4.37 (8H, m, 4 α -OCH₂); 3.67–4.07 (8H, m, 4 β -OCH₂). ¹³C-NMR (CDCl₃) (Fig. 3); δ (mg l⁻¹): 144.84; 133.65; 132.40; 129.80; 129.32; 128.49; 128.07; 127.69; 127.50; 126.99; 126.59; 123.58; 121.30; 119.51; 118.33; 113.97; 68.10; 70.50. CHNS-Elemental Analysis; C: 67.20% (calculated: 67.91%); H: 5.81% (calculated: 5.70%); N: 5.40% (calculated: 5.28%). ESI – MS: (m/z) [M+1]⁺ = 531; [M+Na]⁺ = 553; 383; 323; 301; 195; 179; 157 (Fig. 4).

Hg²⁺ ion recognition in aqueous buffer solution

Stock solutions (10 mM) of nitrates of Hg²⁺, Li⁺, Na⁺, Ag⁺, Pb²⁺, K⁺, Mg²⁺ and Ni²⁺ as well as chlorides of Zn²⁺, Cu²⁺, Sr²⁺ and Ca²⁺ were prepared in Titrisol aqueous buffer solution (pH 7). The DB18C6 naphthyl azo dye stock solution of 0.1 mM was prepared in 1:1 MeOH/H₂O solution since the dye was not completely soluble in water.

- **Test solutions:** 4 ml of the dye stock solution and 0.5 ml of the metal stock solution was added to 13 separate test tubes. The test tubes were then shaken for 1 h before fluorescence measurements were taken.
- **Titration experiments:** 4 ml of the dye stock solution was added into a cuvette. Small volumes (5 μ l – 200 μ l) of metal

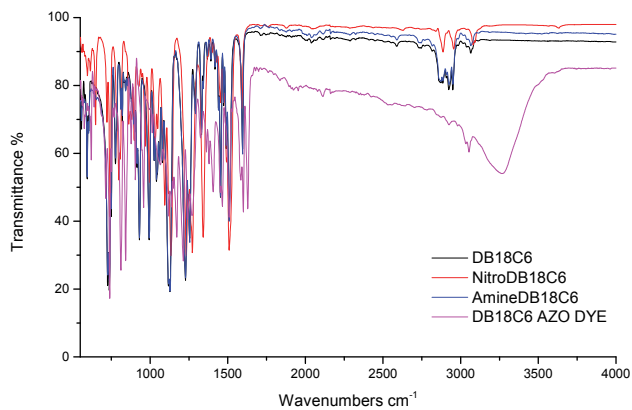


Figure 3
FT-IR spectra of dye sensor (DB18C6 AZO DYE) starting material (DB18C6) and intermediates (NitroDB18C6 and AmineDB18C6)

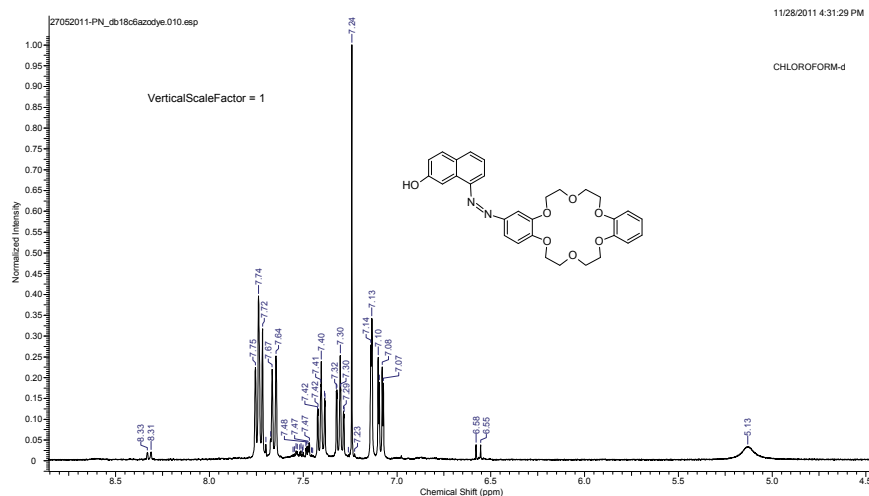


Figure 4
¹H-NMR spectrum of the dye sensor molecule (solvent: CDCl₃)

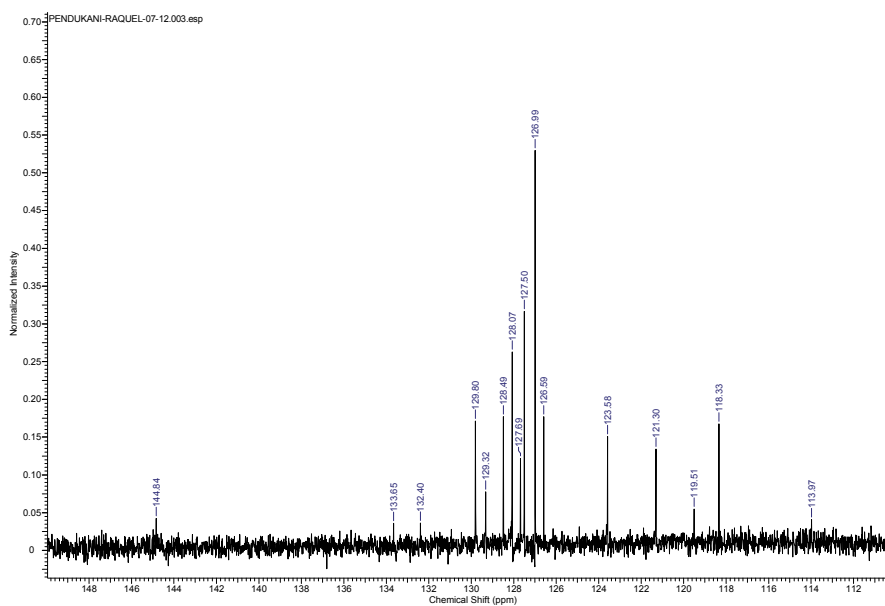


Figure 5
¹³C-NMR spectrum of the dye sensor molecule (solvent: CDCl₃)

(Cu²⁺ and Hg²⁺) were added and a fluorescence spectrum was taken after each addition. The volumes added corresponded to metal ion concentrations in the range 0 to 3 × 10⁻³ M.

Water sample

The water sample was collected from a stream next to a power generation station in Johannesburg. The pH and conductivity of the sample were taken using a pH meter. The dissolved organic content (DOC) of the water sample was determined using a total organic carbon (TOC) analyser (Teledyne Tekmar, TOC fusion). Samples were first filtered through a 0.45 μm membrane filter to remove any suspended solids. The sample was then digested using nitric acid to remove all dissolved organics before the concentrations of selected metal ions were determined by inductively coupled plasma optical emission spectroscopy (ICP-OES).

RESULTS AND DISCUSSION

Synthesis and characterisation of the sensor molecule

The dye sensor molecule was characterised by UV-Vis spectrophotometry, FT-IR, ¹H-NMR, ¹³C-NMR, ESI-MS and elemental analysis. The UV-Vis absorption spectrum (1.0 mM in ethanol/water 1:1 mixture) is shown in Fig. 2(a); Fig. 2(b) gives the fluorescence emission spectrum of the dye. The dye had a maximum absorbance at 380 nm and a fluorescence emission maximum at 432 nm.

From the FT-IR spectrum (Fig. 3) of the dye sensor molecule the appearance of the OH-stretching band at 3 265 cm⁻¹, along with the C–O–C stretch around 1 241 cm⁻¹ confirmed the formation of the dye containing the crown ether and the naphthyl part. Further characterisation using ¹H-NMR (Fig. 4) and ¹³C-NMR (Fig. 5) confirmed the structure of the dye.

The calculated molecular mass of the dye sensor from the proposed structure in Fig. 1 is 530.58 g·mol⁻¹. This was confirmed from the mass spectrum of the product (Fig. 6) with the appearance of peaks at m/z = 531 corresponding to the [M + 1]⁺ ion and the peak at m/z = 553 due to the [M + Na]⁺ ion, from the sodium used in the electrospray ionisation (ESI) method to obtain the spectrum. The fragmentation pattern seen in the spectrum was also consistent with the proposed structure, notably the peak at m/z = 383 corresponding to the fragment [DB18C6 + Na]⁺ ion.

From the calculated molecular mass the percentage composition is

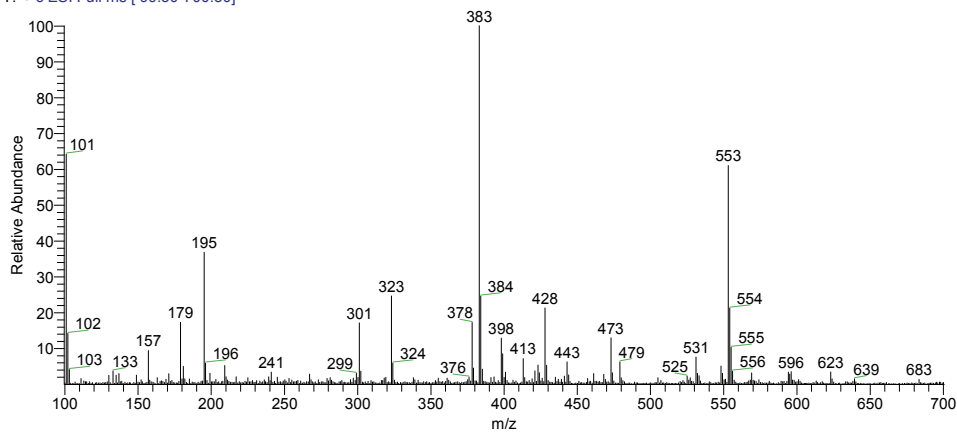


Figure 6
ESI-MS spectrum of the dye sensor molecule

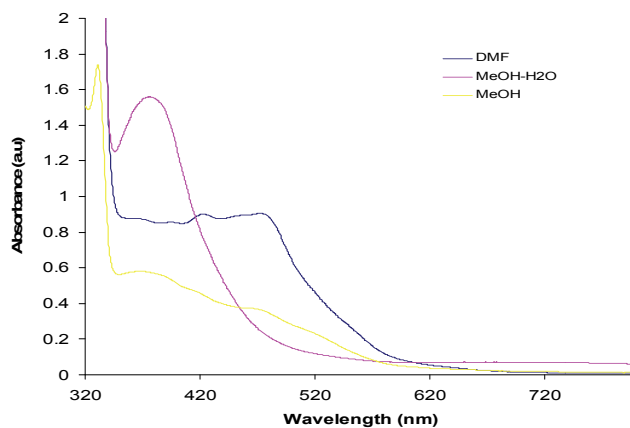


Figure 7

Effect of solvents on the absorption of dye sensor molecule

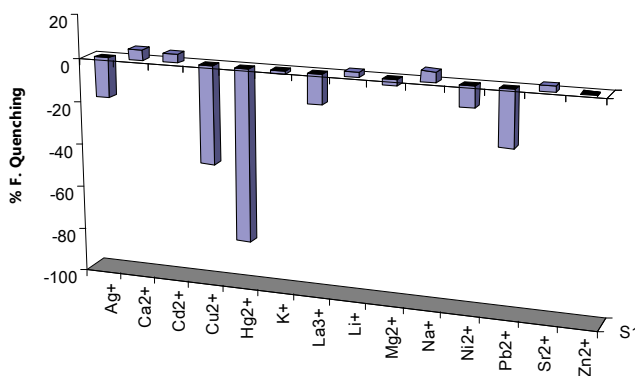


Figure 9

Percentage fluorescence quenching of DB18C6 azo dye due to adding various metal ions

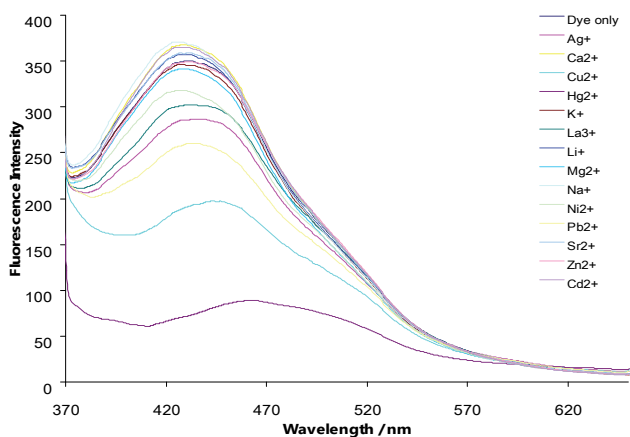


Figure 8

Effect of adding various metal ions (M^{n+}) on fluorescence of DB18C6 azo dye. $[M^{n+}] = 1.0 \text{ mM}$; $[DB18C6 \text{ dye}] = 10^{-4} \text{ M}$.

C: 67.91%; H: 5.70%; N: 5.28%. This was confirmed from the results of elemental analysis of the product which were close to the calculated values (C: 67.20%; H: 5.81%; N: 5.40%).

Hg²⁺ ion recognition by fluorescence emission spectroscopy

The absorption of the dye in different solvents was investigated

(Fig. 7). It was observed that in a mixture of methanol and water the dye gave the highest absorption and a well-defined absorption maximum, whereas a broad absorption band was seen with, for example, DMF. A 1:1 mixture of methanol and water was therefore chosen as the solvent for the rest of the analyses.

The absorption spectrum of the DB18C6-dye was not changed by the addition of metal ions. The sensing of metal ions by the dye was therefore studied by fluorescence spectroscopy. The fluorescence spectrum of the dye in a 1:1 MeOH/H₂O solution is shown in Fig. 2(b).

The emission spectra of the DB18C6-dye in the absence and presence of 14 different metal ions (Ag⁺, Ca²⁺, Cu²⁺, Hg²⁺, K⁺, La³⁺, Li⁺, Mg²⁺, Na⁺, Ni²⁺, Pb²⁺, Sr²⁺, Zn²⁺ and Cd²⁺) were recorded separately and plotted on the same axes (Fig. 8). Addition of Hg²⁺ ions (1.0 mM) resulted in the greatest quenching of fluorescence of the DB18C6-dye (75%) while other metal ions resulted in only slight quenching or slight fluorescence enhancement, except for Cu²⁺ (45%) and Pb²⁺ (30%) (Fig. 9). Changes resulting from all other metals were insignificant (all <6%) compared to a 75% quenching for Hg²⁺ ions. Interference in the sensing of Hg²⁺ ions could therefore only be expected from Cu²⁺ and Pb²⁺ when using the proposed sensing probe, and similar observations have been previously reported for similar types of sensing materials (Hsieh et al., 2009; Hu et al., 2010). It is therefore important to ensure that levels of Cu²⁺ and Pb²⁺ are low in a water sample when applying this sensing method.

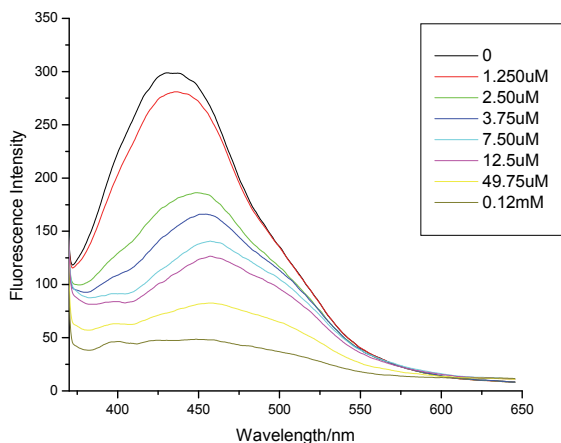


Figure 10

Hg²⁺ titration ($\lambda_{exc} = 355 \text{ nm}$; $[\text{Hg}^{2+}] = 0$; 1.25 μM to 0.12 mM)

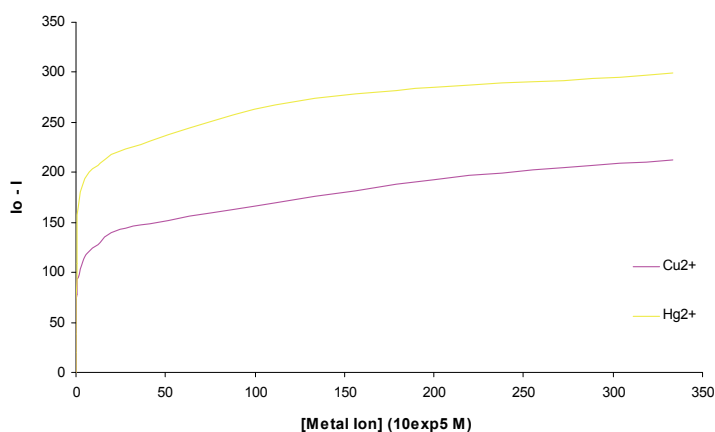


Figure 12

Fluorescence change ($I_0 - I$) as a function of metal ion concentration

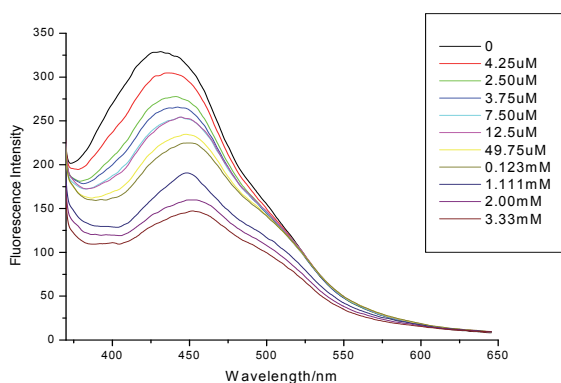


Figure 11

Cu²⁺ titration ($\lambda_{exc} = 355 \text{ nm}$; $[\text{Cu}^{2+}] = 4.25 \mu\text{M}$ to 3.3 mM)

In Fig. 8 it can be seen that in the presence of Hg²⁺ ion, in addition to fluorescence quenching, there was also a red shift of 29 nm, from 432 nm in the absence of Hg²⁺ to 461 nm after 1.0 mM Hg²⁺ was added. This shift can be attributed to the effective change in the conjugation of the crown ether as a result of its complexation with the Hg²⁺ ion (Yari and Papi, 2009). The shift suggests that the interaction between Hg²⁺ and the dye involves the transfer of electrons between the excited naphthyl fluorophore and the metal ion-crown ether complex (Hsieh et al., 2009). For all the other metal ions only insignificant shifts ($\pm 3 \text{ nm}$) were observed, except for Cu²⁺ which resulted in a 15 nm red shift (see Fig. 8), confirming significant complexation of Cu²⁺ with the probe and therefore possible interference.

Titration experiments

To gain further insight into the interaction of the dye with

the metal ions, titration experiments were carried out. Hg²⁺ and Cu²⁺ were chosen as they gave the highest fluorescence quenching.

Figures 10 and 11 show the titration results for Hg²⁺ and Cu²⁺, respectively. Increasing the concentration of Hg²⁺ resulted in an increase in the fluorescence quenching. The fluorescence is quenched to the instrument noise level ($I = 40$) after adding $1.2 \times 10^{-4} \text{ M}$ Hg²⁺, while even after adding a 30-fold concentration of Cu²⁺ ($3.33 \times 10^{-3} \text{ M}$) there was only a 50% fluorescence quenching. This shows great sensitivity of the dye towards Hg²⁺ ions. Figure 6 shows that for mercury a very high level of quenching is reached at very low concentrations of Hg²⁺ compared to Cu²⁺, demonstrating greater sensitivity towards the former. The lowest detectable amount of Hg²⁺ ion was determined from the titration plots to be $1.25 \times 10^{-8} \text{ M}$. This limit compared favourably to similar types of sensing materials (Table 1).

Binding constants and stoichiometry of interaction

The binding constants (K_{sv}) for the interaction of the Hg²⁺ and Cu²⁺ with the dye material were determined from Stern-Volmer Plots. The constants were calculated using the Stern-Volmer equation (Keizer, 1983):

$$I_0/I = K_{sv} [Q] + 1$$

where:

- I_0 = fluorescence intensity in absence of added quencher
- I = fluorescence intensity in presence of added quencher
- $[Q]$ = concentration of quencher
- K_{sv} = quenching constant

Sensing material	Medium	pH	Detection limit (M)	Binding constant (M ⁻¹)	Major interference	Reference
Sugar-azo-crown ether	Methanol	-	1.39×10^{-5}	4.0×10^5	Cu ²⁺	Hsieh et al., 2009
Bovine serum albumin capped gold nanoparticles	Water	7.4	7.90×10^{-8}	-	Cd ²⁺ , Zn ²⁺ , Cu ²⁺ , Ni ⁺	Hu et al., 2010
p-Dimethylamino benzaldehyde thiosemicarbazone	Ethanol/water	4.6	7.7×10^{-7}	7.48×10^6	Cu ²⁺	Yu et al., 2010
Dibenzo-18-crown-6 ether azo dye	Water	4	1.25×10^{-8}	1.0×10^5	Cu ²⁺	This work

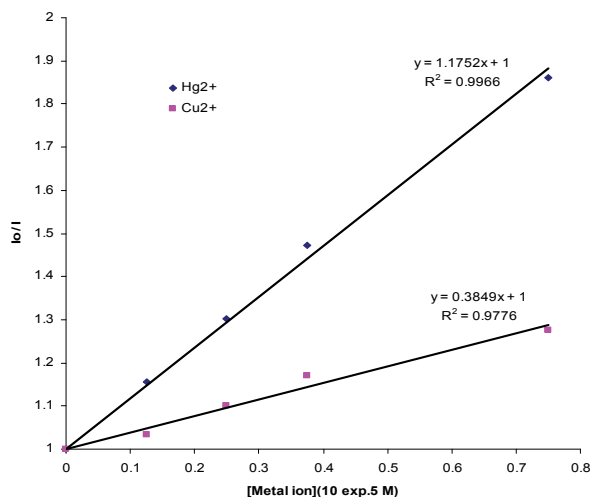


Figure 13
Stern-Volmer Plots

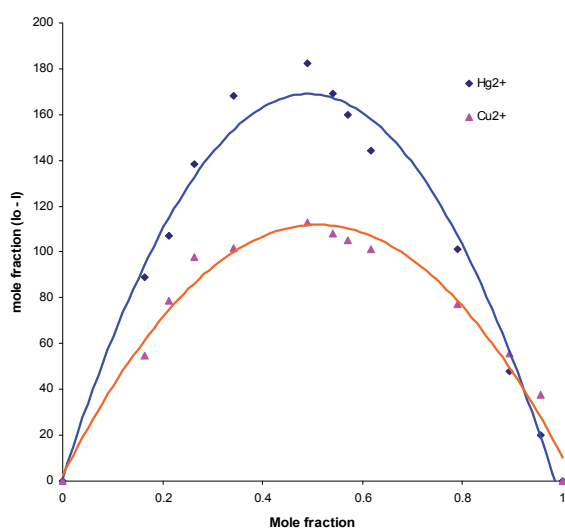


Figure 14
Job plots

From the plot (Fig. 13), the slopes of the linear fits gave Stern-Volmer quenching constants of $1.18 \times 10^5 \text{ M}^{-1}$ and $3.85 \times 10^4 \text{ M}^{-1}$ for Hg²⁺ and Cu²⁺, respectively. The three-fold higher constant for Hg²⁺ suggests that a much stronger complex is formed between the Hg²⁺ ion and the crown moiety of the DB18C6 dye, as compared to the Cu²⁺ complex. The binding constants are comparable to those reported elsewhere (Hsieh et al., 2009; Hu et al., 2010), confirming that an Hg²⁺-DB18C6-dye complex had indeed been formed (Table 1).

To determine the stoichiometry of the complexation process between the metal ions and the dye ligand, Job plots were made (Fig. 9). In the plots the x-axis is the mole fraction, the ratio of the concentration of the metal ion to the total concentration of the dye and metal ion. The total molar concentration of the dye and metal ion were kept constant at $1.00 \times 10^{-4} \text{ M}$. The stoichiometry of the complexation process is obtained from the plot by noting the mole fraction that gives the maximum fluorescence response (Chen et al., 2013). From Fig. 14 the stoichiometries of both Hg²⁺ and Cu²⁺ are 1:1 as the maximum of both plots is at 0.5.

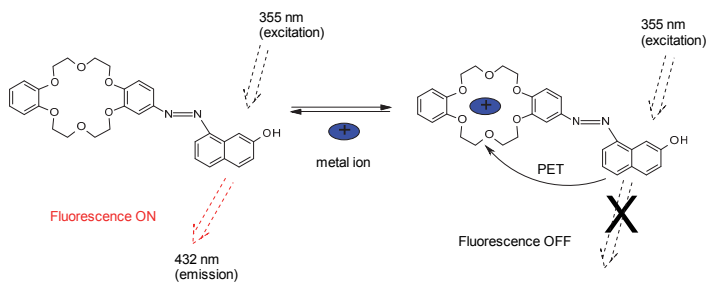


Figure 15
Proposed mechanism for fluorescence quenching

Dibenzo-18-crown-6-ethers have been shown in earlier work to form complexes with Hg²⁺ ions (Williams et al., 2009). The quenching of fluorescence observed upon addition of Hg²⁺ ions can be attributed to the reverse photo-induced electron transfer (PET) mechanism involving electron donation from the excited naphthyl azo fluorophore part to the metal ion complexed crown ether receptor part (He et al., 2009) as illustrated in Fig. 15. Before the addition of Hg²⁺ ion, excitation of the fluorophore with UV radiation (355 nm) resulted in the emission of red light (432 nm). After the metal ion had been added, the excited electron from the fluorophore was transferred to the metal-bound crown ether part which acted as an electron acceptor resulting in no fluorescence being observed (Fig. 15). This mechanism was further supported by the fact that no change in the absorption spectra was observed, meaning that the quenching could only be due to the interaction between the fluorophore in the excited state as the donor and the bound metal ion as the acceptor (Motoshiya et al., 2008).

Interference from other metal ions

To investigate interference from other metals on the fluorescence quenching of the dye by Hg²⁺, all metal ions were added to the dye solution except Hg²⁺. In the absence of Hg²⁺ fluorescence quenching was only about 40% (Fig. 16), most of which could be attributed to Cu²⁺ ions. In the presence of Hg²⁺, however, a significant quenching was observed, even in the presence of the other metals. This should provide a means for detecting Hg²⁺ in solution, based on the decrease in fluorescence even in the presence of other interfering ions.

ANALYSIS OF REAL WATER SAMPLE

The proposed sensing probe was tested on an industrial water sample obtained from a power generation plant that uses coal, with a high probability of mercury release into both the atmosphere and water. The physical properties and concentrations of selected metal ions in the water sample as collected are shown in Table 2.

Dissolved organic content was found to be $4.82 \text{ mg}\cdot\ell^{-1}$ (Table 2) and so the water sample was first digested with concentrated HNO₃ to remove any organic species that could interfere with the fluorescence analysis. The concentration of metal ions in the water sample were so low that they would not be expected to interfere with the method, since, from Fig. 6, concentrations as high as $1.0 \times 10^{-3} \text{ M}$ showed no significant quenching of fluorescence of the dye sensor. Notably the concentration of Cu²⁺, a likely interference, was very low ($6.83 \times 10^{-5} \text{ M}$), and therefore the sample was analysed with the

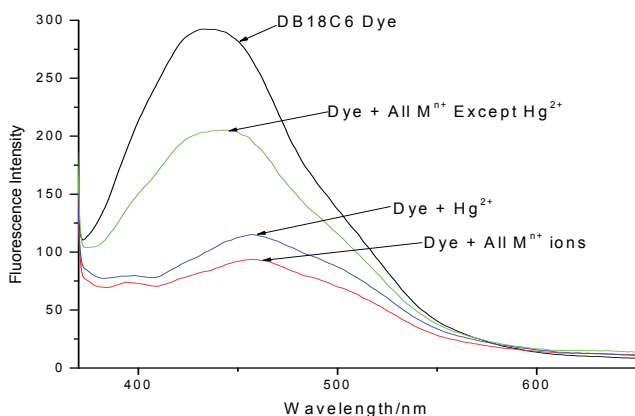


Figure 16

Effect of other metals on Hg^{2+} fluorescence quenching of DB18C6 azo dye. $[\text{Hg}^{2+}] = 1 \times 10^{-4} \text{ M}$; [other metal ions] = $3.0 \times 10^{-3} \text{ M}$

Property	Value
pH	6.7
Conductivity ($\text{mS}\cdot\text{cm}^{-1}$)	0.1
Dissolved organic content (DOC) ($\text{mg}\cdot\text{l}^{-1}$)	4.82
Hg^{2+} ($\text{mol}\cdot\text{l}^{-1}$)	$1.65 \times 10^{-6} \pm 0.01$
Cu^{2+} ($\text{mol}\cdot\text{l}^{-1}$)	$6.83 \times 10^{-5} \pm 0.05$
Na^+ ($\text{mol}\cdot\text{l}^{-1}$)	$7.50 \times 10^{-3} \pm 0.01$
K^+ ($\text{mol}\cdot\text{l}^{-1}$)	$1.05 \times 10^{-4} \pm 0.04$
Ca^{2+} ($\text{mol}\cdot\text{l}^{-1}$)	$2.65 \times 10^{-5} \pm 0.01$
Mg^{2+} ($\text{mol}\cdot\text{l}^{-1}$)	$7.06 \times 10^{-5} \pm 0.01$
Ag^+ ($\text{mol}\cdot\text{l}^{-1}$)	$7.22 \times 10^{-5} \pm 0.01$
Pb^{2+} ($\text{mol}\cdot\text{l}^{-1}$)	$5.35 \times 10^{-6} \pm 0.02$

Water sample	Spike level (10^6 M)	$[\text{Hg}^{2+}]$ (10^6 M) by proposed method	$[\text{Hg}^{2+}]$ (10^6 M) by ICP-OES
Unspiked tap water	-	-	-
Tap water A	2.0	1.95 ± 0.03	2.03 ± 0.02
Tap water B	5.0	4.89 ± 0.05	5.00 ± 0.03
Industrial water	-	1.64 ± 0.05	1.65 ± 0.01
Industrial water	2.0	3.64 ± 0.03	3.65 ± 0.02

proposed method without any further treatment. A portion of the industrial water sample was also spiked with a known amount of Hg^{2+} along with 2 tap water samples. The concentration of Hg^{2+} in the four water samples was determined from a calibration curve, plotting quenching efficiency, $(I_0 - I)/I_0$ versus $[\text{Hg}^{2+}]$ (Hu et al., 2010). The results obtained were confirmed by inductively coupled plasma optical emission spectrometry (ICP-OES) (Table 3).

The concentration of mercury (II) in the industrial sample was found to be $1.64 \times 10^{-6} \text{ M}$ ($0.33 \text{ mg}\cdot\text{l}^{-1}$) and this was confirmed by ICP-OES. Furthermore the determination of spiked water samples produced results which were in agreement with the well-established ICP method (Table 2). The presence of other metals ions at concentrations shown in Table 2, therefore,

showed no interference with the method, since the amount of Hg^{2+} was determined to a high degree of accuracy in comparison to the ICP method.

CONCLUSION

A simple sensor molecule was synthesised, characterised and used for the fluorescent detection of Hg^{2+} ions. Its applicability in actual samples showed that the molecule can be used for the detection of Hg^{2+} as a simple measure for determining water quality. The results reported show the photo-induced electron transfer (PET) resulting from the complexation of Hg^{2+} with a crown moiety of a crown-ether modified azo dye. The dye can be used as a probe for selective mercury (II) ion detection in water samples. The dye is easily prepared, has a low detection limit, is sensitive and has a rapid response time. No interference effects of other metal ions commonly found in water were observed in the response of the dye to mercury (II) ions. The dye was successfully used to detect Hg^{2+} ions in an industrial water sample and to determine the amount of mercury in the samples. The probe dye material can be attached or mixed with other materials for incorporation into sensing devices.

ACKNOWLEDGMENTS

The authors wish to thank the National Research Foundation (NRF), South Africa, and the Faculty of Science, University of Johannesburg, for funding this work.

REFERENCES

- ABU-SHAWISH HM (2009) A mercury (II) selective sensor based on N,N'-bis(salicylaldehyde)-phenylenediamine as neutral carrier for potentiometric analysis in water samples. *J. Hazardous Mater.* **167** 602–608.
- CHEN X, JOU MJ, LEE H, KOU S, LIM J, NAM S-H, PARK S, KIM K-M and YOON J (2009) New fluorescent and colorimetric chemosensors bearing rhodamine and binaphthyl groups for the detection of Cu^{2+} . *Sensors & Actuators B: Chem.* **137** 597–602.
- DABROWSKI JM, ASHTON PJ, MURRAY K, LEANER JJ and MASON RP (2008) Anthropogenic mercury emissions in South Africa: Coal combustion in power plants. *Atmos. Environ.* **42** (27) 6620–6626.
- FAKHARI AR, GANJALI MR and SHAMSIPUR M (1997) PVC-based hexathia-18-crown-6-tetraone sensor for mercury (II) ions. *Anal. Chem.* **69** 3693–3696.
- FUJIKI M AND TAJIMA S (1992) The Pollution of Minamata Bay by mercury. *Water Sci. Technol.* **25** (11) 133–140.
- GREBENYUK AD, ANDREEV SA, STEPNEVSKAYA IA, LEVKOVICH MG and TASHMUKHAMEDOVA AK (2000) Nitration of benzo crown ethers with potassium nitrate in polyphosphoric acid. *Chem. Heterocycl. Compds.* **36** (12) 1449–1456.
- GUO X, QIAN X and JIA L (2004) A highly selective and sensitive fluorescent chemosensor for Hg^{2+} in neutral buffer aqueous solution. *J. Am. Chem. Soc.* **126** 2272–2273.
- HE C, ZHU W, XU Y and QIAN X (2009) Trace mercury (II) detection and separation in serum and water samples using a reusable bifunctional fluorescent sensor. *Anal. Chim. Acta* **651** 227–233.
- HSIEH Y-C, CHIR J-L, WU H-H, CHANG P-S and WU A-T (2009) A sugar-aza-crown ether-based fluorescent sensor for Hg^{2+} and Cu^{2+} . *Carbohydr. Res.* **344** 2236–2239.
- HU D, SHENG Z, GONG P, ZHANG P and CAI L (2010) Highly selective fluorescent sensors for Hg^{2+} based on bovine serum albumin-capped gold nanoclusters. *Analyst* **135** 1411–1416.
- KEIZER J (1983) Nonlinear fluorescence quenching and the origin of positive curvature in Stern-Volmer plots. *J. Am. Chem. Soc.* **105** 1494–1498.

- KHANI H, ROFOUEI MK, ARAB P, GUPTA VK and VAFAEI Z (2010) Multi-walled carbon nanotubes-ionic liquid-carbon paste electrode as a super selectivity sensor: Application to potentiometric monitoring of mercury ion(II). *J. Hazardous Mater.* **183** 402–409.
- KIWAN AM, EL-SHAHAWI MS, ALDHHAHERI SM and SALEH MH (1997) Sensitive detection and semiquantitative determination of mercury (II) and lead (II) in aqueous media using polyurethane foam immobilized 1,5-di-(2-fluorophenyl)-3-mercaptopformazan. *Talanta* **45** 203–211.
- KONDO S, TAKAHASHI T, TAKIGUCHI Y and UNNO M (2010) Synthesis and photophysical properties of a 2,2'-bianthracene-based receptor bearing two aza-15-crown-5 ethers for naked-eye detection of barium ion. *Tetrahedron Lett.* **52** 453–457.
- KUDO A, FUJIKAWA Y, MIYAHARA S, ZHENG J, TAKIGAMI H, SUGAHARA M and MURAMATSU T (1998) Lessons from Minamata mercury pollution, Japan – after a continuous 22 years of observation. *Water Sci. Technol.* **38**(7) 187–193.
- LEE D-N, KIM G-J and KIM H-J, (2009) A fluorescent coumarinyl-alkyne probe for the selective detection of mercury (II) ion in water. *Tetrahedron Lett.* **50** 4766–4768.
- MARTINIS EM, BERTÓN P, OLSINA RA, ALTAMIRANO JC and WUILLOUD RG (2009) Trace mercury determination in drinking and natural water samples by room temperature ionic liquid based-preconcentration and flow injection-cold vapor atomic absorption spectrometry. *J. Hazardous Mater.* **167** 475–481.
- MOCZAR I, HUSZTHY P, MEZEI A, KADAR M and NYITRAI J (2010) Synthesis and optical characterization of novel azacrown ethers containing an acridone or an N-methylacridone unit as potential fluorescent chemosensors. *Tetrahedron* **66** 350–358.
- MOTOYOSHIYA J, FENGQIANG Z, NISHII Y and AOYAMA H (2008) Fluorescence quenching of versatile fluorescent probes on strongly electron-donating distyrylbenzenes responsive to aromatic chlorinated and nitro compounds, boronic and Ca²⁺. *Spectrochim. Acta: A.* **69** 167–173.
- NCUBE P, KRAUSE RW and MAMBA BB (2011) Fluorescent sensing of chlorophenols in water using an azo dye modified β -cyclodextrin polymer. *Sensors* **11** 4598–4608.
- PACYNA EG, PACYNA JM, STEENHUISEN F and WILSON S (2006) Global anthropogenic mercury emission inventory for 2000. *Atmospheric Environment* **40** 4048–4063.
- PANDYA BR and AGRAWAL YK (2002) Synthesis and characterization of crown ether based azo dyes. *Dyes Pigments* **52** 161–168.
- PASSARIELLO B, BARBARO M, QUARESIMA S, CASCIELLO A and MARABINI A (1996) Determination of mercury by inductively coupled plasma–mass spectrometry. *Microchem. J.* **54** (4) 348–354.
- WILLIAMS NJ, HANCOCK RD, RIEBENSPIES JH, FERNANDES M and DE SOUSA AS (2009) Complexation of mercury(I) and mercury(II) by 18-crown-6: hydrothermal synthesis of the mercuric nitrite complex. *Inorg. Chem.* **48** (24) 11724–11733.
- YANG F, LIU R, TAN Z, WEN X, ZHENG C and LV Y (2010) Sensitive determination of mercury by a miniaturized spectrophotometer after in situ single-drop microextraction. *J. Hazardous Mater.* **183** 549–553.
- YARI A and PAPI F (2009) Highly selective sensing of mercury (II) by development and characterization of a PVC-based optical sensor. *Sensors Actuators B: Chem.* **138** 467–473.
- YU Y, LIN L-H, YANG K-B, ZHONG X, HUANG R-B and ZHENG L-S (2006) *p*-Dimethylaminobenzaldehyde thiosemicarbazone: A simple novel selective and sensitive fluorescent sensor for mercury (II) in aqueous solution. *Talanta* **69** (1) 103–106.